Adsorption of Aromatics in MFI-Type Zeolites: Experiments and Framework Flexibility in Monte Carlo Simulations

Caro-Ortiz, S.; Zuidema, E.; Dekker, D.; Rigutto, M.; Dubbeldam, D.; Vlugt, T.J.H.

Link to publication

Article

Adsorption of Aromatics in MFI-Type Zeolites: Experiments and Framework Flexibility in Monte Carlo Simulations

Sebastián Caro-Ortiz, Erik Zuidema, Desmond Dekker, Marcello Rigutto, David Dubbeldam, and Thijs J. H. Vlugt*

Read Online

ACCESS | Metrics & More | Article Recommendations | Supporting Information

ABSTRACT: Computer simulations of adsorption of aromatics in zeolites are typically performed using rigid zeolite frameworks. However, adsorption isotherms for aromatics are very sensitive to small differences in the atomic positions of the zeolite (*Chem. Phys. Lett.*, **1999**, *308*, 155−159). This article studies the effect of framework flexibility on the adsorption of aromatics in MFI-type zeolites computed by grand-canonical Monte Carlo simulations. New experimental data of adsorption of ethylbenzene in a MFI-type zeolite at 353 K is presented. The adsorption of *n*-heptane, ethylbenzene, and xylene isomers is computed in three MFI-type zeolite structures. It is observed that the intraframework interactions in flexible framework models induce small but important changes in the atom positions of the zeolite and hence in the adsorption isotherms. Framework flexibility is differently "rigid": flexible force fields produce a zeolite structure that vibrates around a new equilibrium configuration with limited capacity to accommodate to a bulky guest molecule. The vibration of the zeolite atoms only plays a role at high loadings, and the adsorption is mainly dependent on the average positions of the atoms. The simulations show that models for framework flexibility should not be blindly applied to zeolites and a general reconsideration of the parametrization schemes for such models is needed.
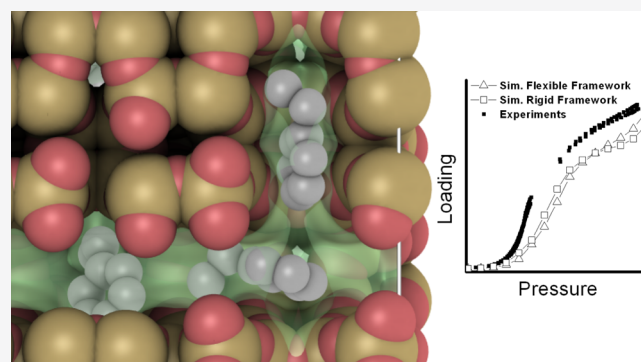
1. INTRODUCTION

Zeolites are versatile materials that have been used for many different applications. The use of zeolites ranges from water cleaning,[1,2] catalyst for the refining industry,[3] to the capture of radioactive particles,[4] among other applications.[5−8] Knowledge of the adsorption behavior of hydrocarbons in the pores of zeolites is important for the understanding of the catalytic activity of the zeolite.[9−11] Many industrial processes, such as the separation of xylenes, disproportionation of toluene, ethylbenzene dealkylation, strongly rely on the interaction of hydrocarbons within a zeolite.[12−15]

Zeolites are commonly considered as very rigid structures as its atomic bonds and angles are highly constrained.[16,17] An inflection point in the adsorption isotherm reflects either that molecules start to fill a new adsorption site[18,19] and/or that there is a structural change in the zeolite due to the number of adsorbed molecules[20−22] or the temperature.[23,24] Adsorption of aromatics in MFI-type zeolites is a typical example of a mix of such factors.[25] Talu et al.[20] described the isotherm shapes for benzene, toluene, and *p*-xylene adsorbed in MFI-type zeolites. It is reported that, with increasing temperature, the isotherm shape changes from type IV to type I.[20] The observable kink in the isotherm at lower temperatures disappears at temperatures higher than 80 °C.[20] The all-silica

form of the MFI-type zeolite (silicalite) is known to show a monoclinic or orthorhombic structure depending on the temperature and loading.[26,27] Van Koningsveld et al.[28] identified three structures of the *p*-xylene/silicalite system: Mono (monoclinic), Ortho (orthorhombic) and Para (also orthorhombic). Very small structural differences are observed between the Ortho and Para lattices.[29] The silicalite/*p*-xylene system is known to have the Ortho structure when the loading is lower than 4 molec./uc.[28] At 8 molec./uc, the silicalite/*p*-xylene system shows the Para structure.[26] Sacerdote et al.[30] reported that silicalite loaded with benzene, toluene, or ethylbenzene shows a Mono structure for loadings lower than 4 molec./uc. Sorenson et al.[31] reported that benzene loading does not cause a significant change in the unit cell volume of silicalite. *o*-Xylene and *m*-xylene do not access nor cause significant deformations to the zigzag channels relative to the room-temperature empty Mono framework.[32] *o*-Xylene is
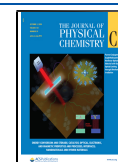
located exclusively in the intersections of the channels at 273 and 315 K.[33] Several experimental studies that describe the adsorption of aromatics in MFI-type zeolites can be found in the literature.[20,26,30,32−45]

The adsorption of aromatics in MFI-type zeolites has also been studied by molecular simulations. Commonly, Monte Carlo (MC) simulations in the grand-canonical ensemble (GCMC) are used to compute sorbate loadings as a function of temperature and pressure in a zeolite framework.[46−48] Several studies where MC is used to investigate adsorption of aromatics in MFI-type zeolites can be found in the literature.[49−62] Snurr et al.[49] computed adsorption isotherms of benzene and *p*-xylene in MFI-type zeolites. Large differences in the loadings are found when using the MFI Ortho and Para structures. It is shown that, below 4 molec./uc, benzene and *p*-xylene are adsorbed in the intersections of the Ortho structure. Molecules in the intersections are too far apart to strongly interact with each other. The molecules are also located in the channels at higher loadings, allowing sorbate/sorbate interactions.[49] Torres-Knoop et al.[51] reported simulations of adsorption of ethylbenzene and styrene in the Para form of MFI-type zeolite at 433 K. It is observed that, close to saturation conditions, styrene can be located in the zigzag channel. At the same conditions, ethylbenzene suffers from size exclusion effects. Therefore, it is located exclusively in the intersections of the channels. Mohanty et al.[52] reported GCMC simulations of *p*-xylene and *m*-xylene in silicalite. These authors found that *p*-xylene adsorption selectivity over *m*-xylene is due to the difficulty of *m*-xylene to access the adsorption sites of the framework in comparison to *p*-xylene. The large energetic difference between *p*-xylene and *m*-xylene is the primary reason for *p*-selectivity.

Computer simulations of the adsorption of hydrocarbons in zeolites are typically performed using rigid zeolite frameworks.[46,63,64] Clark and Snurr[65] performed simulations of the adsorption of benzene in the Ortho and Para structures of silicalite at 343 K. The simulations showed that the computed loadings are very sensitive to small differences in the atom positions of the zeolite. It is found that the Henry coefficient of benzene in the Ortho structure described by Olson et al.[66] is 3.1 times larger than in the Ortho structure described by van Koningsveld et al.[67] The mean and maximum differences of the atomic positions of these two Ortho structures are only 0.11 and 0.41 Å, respectively. It is suggested that interactions that include lattice flexibility and polarizability are required to simulate systems where molecules fit tightly in the pores.[65,68]

Only a limited amount of studies have approached the simulations of adsorption using a flexible zeolite framework. García-Pérez et al.[69] and Sánchez-Gil et al.[70] studied argon adsorption in MFI and MEL, respectively.[71] described the loadings of methane in LTA. Fang et al.[72] considered framework flexibility for the adsorption of CO_2 in an ammonium MFI-type zeolite. It is observed that the overall effect of framework flexibility is small for the adsorption of CO_2 in the zeolite structure. Vlugt et al.[63,67] reported the effect of flexibility in the adsorption of *n*-alkanes and cycloalkanes in a MFI-type zeolite. It is found that for molecules with an inflection behavior in the isotherm, the influence of the flexibility seems to be larger than for molecules without such inflection. The influence of the flexibility on the adsorption of cyclohexane is similar to *n*-alkanes.[73]

Framework flexibility has also been studied in other porous materials.[74−80] Witman et al.[81] studied the effect of framework flexibility on the separation of Xe/Kr mixtures in ∼3000 metal−organic frameworks (MOFs). A model that predicts the Henry regime adsorption of each framework and selectivity as a function of framework flexibility is used. The results of this study suggest that the selectivity of the Xe/Kr mixtures can be increased or decreased up to two orders of magnitude when unit cell volume changes are allowed.[81] Agrawal and Sholl[82] examined the adsorption of nine molecules and four mixtures in 100 MOFs. It is observed that adsorption selectivities can be significantly affected by framework flexibility. It is suggested that including framework flexibility is important when attempting to make quantitative predictions of adsorption selectivity in MOFs. Heinen and Dubbeldam[83] review in depth the prospects of development of force fields for framework flexibility in MOFs. In this review, it is shown that there is an urgent need for efficient sampling schemes that capture stimuli-driven phase transitions. This limits the predictive capacity of existing force fields for framework flexibility in MOFs.[83]

This article explores how the inclusion of framework flexibility in a model affects the adsorption of aromatic hydrocarbons in MFI-type zeolites. Structural changes of MFI-type zeolites (i.e., Mono to Ortho/Para transition) imply small geometry and volume changes in the framework unit cell[31,84] that are not considered in this work. Instead, framework flexibility aims to study local changes of the MFI-type zeolite framework induced by the presence of guest molecules. Computations of adsorption of *n*-heptane, ethylbenzene, and xylene isomers are performed in three MFI-type zeolite structures. Several models are considered to describe the flexibility of the zeolite framework. The simulations of *n*-heptane adsorption aim to investigate if the details of framework flexibility play any role on a system known to be well reproduced with a rigid zeolite structure.[85] Experimental data of adsorption of ethylbenzene in a MFI-type zeolite at 353 K is presented. The new experimental data shows higher loadings than in previously reported isotherms in the literature. Pore size distributions are computed to investigate the effect that framework flexibility induces in the MFI-type zeolite structures. The experimental and simulation procedure are explained in Section 2. The results of experiments, computed pore-size distributions, and computed loadings are reported and discussed in Section 3. It is shown that the intraframework interactions in flexible framework models induce small but important changes in the atom positions of the zeolite and hence in the adsorption isotherms. The current challenges to model and predict reliable molecular insights about the system are also discussed in Section 3. Our concluding remarks regarding the influence of the force fields for framework flexibility on the adsorption of aromatics in MFI-type zeolites are discussed in Section 4.

2. METHODS

2.1. Experimental Procedure. Large-crystal ZSM-5 samples with silica-to-alumina ratios of around 80 are synthesized according to established literature procedures.[86] Vapor-phase adsorption isotherms are measured using the volumetric technique on a Micromeritics 3Flex physisorption analyzer. A vapor reservoir filled with ethylbenzene is held at constant temperature at 30 °C through a heating mantle. The adsorbate is purified using the freeze−pump−thaw method to evacuate non-condensed species. The vapor reservoir is immersed in a cryogenic bath. Nitrogen and oxygen are not

condensed at the pressures of the purification process. Nitrogen and oxygen are removed by evacuation. After purification, the sample is maintained at 30 °C. The vapor pressure is determined for this temperature.

About 150−500 mg of the adsorbent powder is placed in a glass sample tube. The zeolites are pre-dried for at least 4 h in vacuum at 450 °C in a Micromeritics SmartVac. The samples are activated in situ in the 3Flex device by increasing the temperature to 450 °C at a heating rate of 10 °C/min under vacuum. The heating mantle is removed and replaced by an external thermostatic bath, maintaining the obtained vacuum ($<5 \times 10^{-5}$ mmHg).

The adsorption isotherms are determined at 80 °C by pressure-controlled dosing of the adsorbate. The partial pressures are increased up to approximately 0.7 $P^{(80 \,°C)}/P_0^{(30°C)}$. The adsorbate is dosed at fixed amounts of 0.2 cm^3/g STP for pressures lower than 0.03 mm Hg. For pressures higher than 0.03 mm Hg, the pressure is increased by a fixed pressure rate of 0.1 mm Hg. The equilibration interval is set at 180 s.

2.2. Simulation Procedure. The adsorption computations are performed using the Continuous Fractional Component Monte Carlo (CFCMC)[87,88] algorithm in the grand-canonical ensemble. The RASPA software[89−91] is used for all simulations. Periodic boundary conditions are applied to a simulation box consisting of 2 × 2 × 3 unit cells of MFI-type zeolite. The all-silica structures described by van Koningsveld et al. (Mono,[84] Ortho,[67] and Para[28]) are considered. The adsorption of aromatics is computed for the three structures. The Ortho structure is used for *n*-heptane adsorption simulations. A cutoff radius of 14 Å is applied for all Lennard-Jones (LJ) interactions, and analytic tail corrections are used.[92,93] The interactions between different atom types are obtained using Lorentz−Berthelot mixing rules.[92] The Ewald summation[94] with a relative precision of 10^{-6} is used to account for the long-range electrostatic interactions. In the CFCMC algorithm, the interactions of a fractional molecule are scaled by the λ parameter in the range of 0−1 (0 for no interactions with surrounding molecules/framework and 1 for full interaction with surrounding molecules/framework).

A MC cycle is the maximum between 20 and *N*-move-attempts, with *N* being the number of molecules in the system.[89] At each MC cycle, trial moves attempt to rotate, displace, randomly reinsert, and insert adsorbates. Also, λ-moves scale the interactions of the fractional molecule (via the CFCMC algorithm[87,88]). The simulations are started with 100,000 MC cycles to initialize the system. The initialization run only allows translation, rotation, and insertion moves. After that, a stage of 400,000 MC cycles is used to equilibrate the system. All the considered types of trial moves are allowed, and the biasing factors for the λ-moves of the CFCMC algorithm are calculated. λ-Moves are biased to obtain a flat λ probability distribution. The use of this move is advantageous as it enables an efficient insertion and deletion of sorbate molecules in the system.[95,96] Ensemble averages are obtained in a 500,000 MC cycles production stage. The reported errors account for the 95% confidence interval calculated by dividing the production run into five parts. An extra MC trial move is included to simulate a flexible zeolite framework, which attempts a random displacement to a randomly selected zeolite atom.[63] Since the volume of the simulation box is fixed, the equilibrium framework density is not affected by framework flexibility.

Force fields that model the flexibility of the zeolite framework (host−host interactions) are commonly based on the description of vibrational properties, such as the infrared spectra of the zeolite atoms,[97,98] and/or ab initio quantum chemical calculations.[99,100] Several force fields for framework flexibility have been reported in the literature.[16,99−107] Such force fields are typically used in the calculations of diffusion of aromatics in MFI-type zeolites by molecular dynamics simulations.[108−110] Some sets of zeolite intraframework interactions only include harmonic potentials between the zeolite atoms, while others also add a combination of LJ and partial charges. Polarization of the zeolite atoms can also be added by using the core−shell method.[111] In this method, typically the oxygen atoms of the zeolite are separated into cores and shells.[112−114] Phase transitions and negative thermal expansion can be studied using this method.[74] The predicted crystal structures agree very well with crystallographic data from experiments.[115] The core−shell model requires formal charges that are higher than the partial charges based on ab initio calculations.[74] The computational time using this method is increased due to the use of more particles in the system.[74]

The Nicholas[105] model, the Demontis[103] model, and the model reported by Jeffroy et al.[16] are considered for investigating the host−host force field induced effects in MFI-type zeolite frameworks. The force field parameters are listed in the Supporting Information. The Demontis model[102−104] consists on describing the flexibility of the zeolite only by Si−O bond stretching and O−Si−O Urey−Bradley potentials. The Nicholas model[105] includes intramolecular (1−4) LJ and electrostatic interactions besides torsional, bond-bending, and bond-stretching potentials. The model by Jeffroy et al.[16] is a transferable force field able to predict the structure of zeolites including extra-framework cations. The host−host interactions are determined by electrostatic interactions, bond-stretching, and bond-angle parameters.

There is a distribution of bond lengths and angles in MFI-type structures from crystallography.[26,67,84] The Nicholas model, the Demontis model, and the model by Jeffroy et al. use constant equilibrium bond lengths and angles. The so-called modified form of these models take the equilibrium bond lengths and bond angles (in the Urey−Bradley term) directly from the crystallographic structure to which the model is applied.[63] As discussed in the following section, this modification is used to avoid large deviations from the experimental crystal structure. In this work, the modified Nicholas[105] model and the modified Demontis[103] model are used for the simulations of adsorption of aromatics.

To take into account the effect that the host−host interactions have on the zeolite structure, an optimization of the atom positions of the zeolite framework at 0 K with the flexible force field is performed. The structure with atom positions optimized is obtained using the mode-following minimization method[116,117] for each initial experimental zeolite topology subject to the host−host force field. The pore-size distribution (PSD) of the structures with atom positions optimized at 0 K using each host−host force field is calculated geometrically with the method of Gelb and Gubbins.[118,119] The MFI-type zeolite atom positions are optimized at 0 K with the Demontis model,[103] the Nicholas model,[105] and the model reported by Jeffroy et al.[16] as well as the modified forms of each force field. The PSD is also
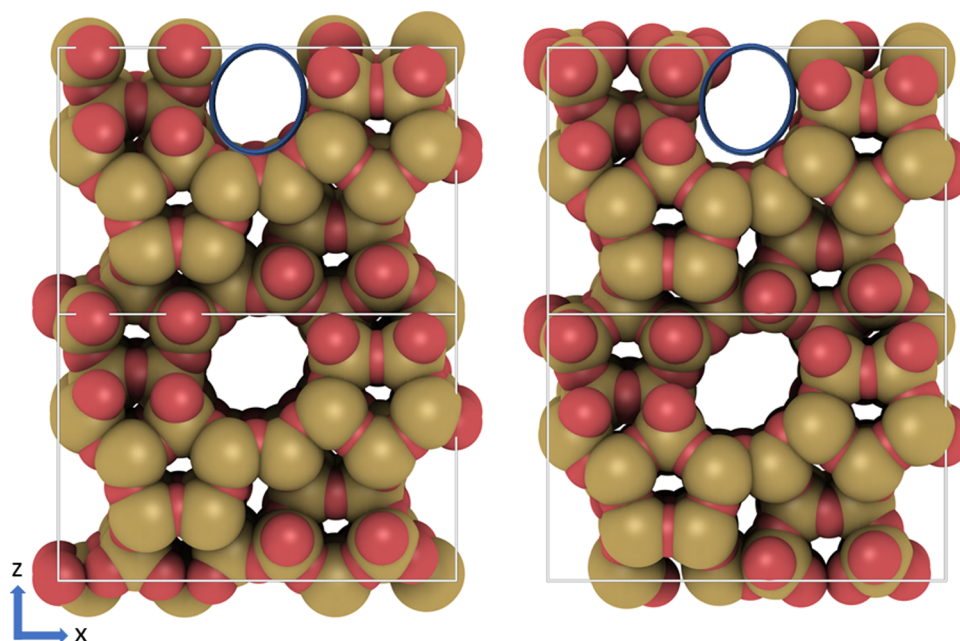
Figure 1. Minimum-energy atomic configuration of MFI Para structures with atom positions optimized at 0 K using the modified Demontis model (left) and the original Demontis[103] model (right). The minimum-energy structure exactly reproduces the experimental crystal structure[28] when using the modified Demontis model. The blue ring is the same in both structures. The blue ring highlights differences in the atomic position and the change of shape of the straight channel caused by the use of fixed equilibrium bond lengths with the original Demontis model.

calculated for each of the MFI-type zeolite lattices from crystallographic data. Henry coefficients of ethylbenzene in the MFI-type structures are calculated via the Widom test-particle insertion method.[120]

The interactions between the zeolite and guest hydrocarbons (host–guest interactions) are described using several force fields.[121–127] The host–guest force fields are usually obtained by fitting the parameters to experimental data,[10] such as adsorption isotherms. The TraPPE-zeo model[126] is used in this work. In this force field, all oxygen and silicon atoms are modeled with Lennard-Jones interactions and partial charges. The development of this force field is focus on transferability and variety of zeolite/guest systems.[126] As such, it is fitted to match the experimental adsorption isotherms of *n*-heptane, propane, carbon dioxide, and ethanol in zeolites. The partial charges of the zeolite atoms are a critical parameter for the force fields and adsorption.[128,129] Typical partial charges for silicon atoms have been reported in the range of +0.5 to +4 e.[130] The host–guest electrostatic interactions from TraPPE-zeo[126] (+1.5 and −0.75 e for Si and O, respectively) are fitted considering fixed positions of the zeolite atoms. Zeolite host–host interactions that include electrostatics are likely to be incompatible with a guest–host force field that also includes electrostatics. The combination of two types of force fields can be cumbersome. The Nicholas model, the Demontis model, and the model reported by Jeffroy et al. use different partial charges for the zeolite atoms than the TraPPE-zeo[126] force field. In this work, the electrostatic interactions of the zeolite atoms are modeled by each host–host force field used in the simulation. The partial charges are listed in the Supporting Information.

Molecular simulations of aromatics typically use force fields (guest–guest interactions) that model the vapor–liquid equilibrium (VLE) with LJ potentials or a combination of LJ and electrostatic interactions.[131,132] In the case of aromatic species, a common practice in the development of these force

fields is to fit the interaction parameters to reproduce the VLE of the pure components[133–139] or by ab initio quantum mechanical calculations.[140–143]

Despite the extensive use of guest–guest force fields that use electrostatic interactions (such as OPLS[138,139]) for the simulation of adsorption of aromatics in zeolites,[49,51,53,144] the electrostatic interactions are fitted for VLE and not for the interaction with a host framework. In this work, the electrostatic interactions of the zeolite atoms are modeled by each host–host force field used in the simulation. Such electrostatic interactions are not suited for the interaction with an adsorbate but for the zeolite framework with itself. Therefore, it is convenient to use a guest–guest force field that does not explicitly use partial charges for electrostatic interaction. The uncharged TraPPE-UA[145,146] force field is chosen for the guest–guest interactions. The TraPPE-UA is a widely used force field that is designed to reproduce the VLE of alkylbenzenes and n-alkanes, among other chemical species. The united atom approach is used by merging a carbon atom and its bonded hydrogen atoms into a single uncharged interaction site representing each CH_x group in the *n*-alkanes and aromatic species. Aromatics are modeled as rigid molecules, except ethylbenzene, that includes a torsional potential in the $CH_3–CH_2–CH$ bond angle. The force field parameters are listed in the Supporting Information.

3. RESULTS AND DISCUSSION

3.1. Force Field Induced Effects in MFI-Type Structures.
The effect of each host–host force field on the zeolite pores can be observed in the pore-size distribution. The PSD of MFI-type zeolite structures with atom positions optimized at 0 K using the Demontis[103] model, the Nicholas[105] model, and the model reported by Jeffroy et al.[16] are calculated. The PSDs are compared with the PSD computed for each experimental crystal structure. The modified form of each force field is also included. As an

example, Figure 1 shows the visible differences in the MFI Para structure when using constant equilibrium bond lengths in the Demontis model compared to the modified Demontis model. For the modified Demontis model, the experimental crystal structure is exactly reproduced when $T \rightarrow 0$ K. With the original Demontis model, atomic positions are shifted and the shape of the straight channel changes to an oval shape. Figure 2 shows the Si−O bond length distribution of the MFI Para
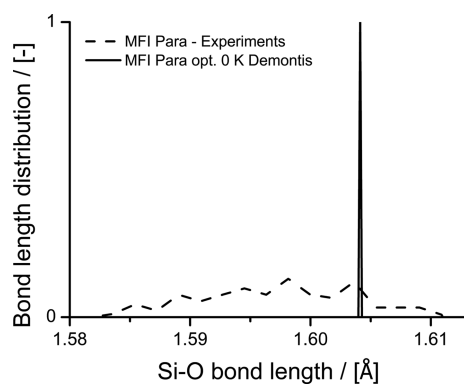

Figure 2. Si−O bond length distribution of the MFI Para from the structure from experiments[28] and from the MFI Para minimum-energy structure obtained optimizing the atomic positions at 0 K using the Demontis[103] model. The original Demontis[103] model uses fixed equilibrium Si−O and O−(Si)−O bond lengths. The Si−O bond length distribution of the MFI Para structure with atom positions optimized at 0 K with the modified Demontis model exactly reproduces the Si−O bond length distribution from experiments.

structure from crystallography[28] and the MFI Para structure with atom positions optimized at 0 K using the original Demontis model. The Si−O bond lengths of MFI Para structure from experiments[28] range from 1.58194 to 1.61089 Å. The Si−O bond length distribution of the MFI Para structure with atom positions optimized using the original Demontis model ranges from 1.60398 to 1.60427 Å. The fixed equilibrium bond lengths of the original Demontis model significantly reduce the bond length range. The shape and atom position changes shown in Figure 1 are caused by the use of fixed equilibrium bond lengths and angles and the reduction of the bond length range. All crystal structures are available in CIF format in the Supporting Information.

The PSD of MFI-type zeolite structures with atom positions optimized at 0 K using the Demontis[103] model, the Nicholas[105] model, and the model reported by Jeffroy et al.[16] are shown in Figure 3. In a PSD of MFI-type zeolites, the peak centered at a diameter of approximately 4 Å corresponds to the zigzag and straight channels. The peak centered at a diameter of approximately 5.5 Å corresponds to the intersection of the channels. Using the Demontis model, significant differences can be observed in the PSD of the Ortho structure. The PSD shows a new peak at a diameter smaller than 4 Å, suggesting that the channels decreased its size. This change in the structure is exclusively related to the use of constant bond lengths and angles. In the Mono and Para structures, the shift of the peak shows that the intersections are smaller.

When the Nicholas model and its modified form are used, the PSDs of the Mono structure do not show significant deviations from the experimental structure. The Nicholas model and the modified form induce an expansion of the intersections in the Ortho structure. The peak corresponding

to the intersection is shifted approximately +0.5 Å. In the Para structure, the peaks corresponding to the intersections and the channels are shifted approximately 1 Å. This means that the pores are significantly larger than in the Para structure from experiments. As the original and modified forms of the Nicholas model show similar shifts of the pore-size peaks, these shifts can be related to the LJ and the strong electrostatic interactions accounted in the optimization of the atom positions with the force field.

The model presented by Jeffroy et al.[16] induces significant differences in the Ortho structure. The channels are smaller, while the intersections are expanded. The peak corresponding to the channels is shifted approximately −0.5 Å. The peak corresponding to the intersections is shifted approximately +0.5 Å. In addition, the intersections of the Para structure approximately 0.5 Å (in diameter) larger than in the crystal structure from experiments. The modified form of this model shows better agreement with the PSD of the experimental Mono and Ortho structures. A mean displacement of 0.462 Å of the atoms in the Para structure suggest that the zeolite structure is significantly influenced by the force field.

Table 1 lists the mean and maximum displacements atomic position induced by each of the host−host force fields and the Henry coefficient of ethylbenzene at 353 K in the MFI-type structures. The displacements suggest that taking the equilibrium bond distances and angles from the experimental crystal structure reduces the deformation induced by the host−host force field in the structure. Clark and Snurr[65] observed that a mean displacement of 0.11 Å of the zeolite atoms is enough to significantly influence the adsorption of benzene in MFI-type zeolites. In this work, all mean displacements accounted in the optimized structures at 0 K with the modified forms of the force fields are higher than 0.11 Å (except for the modified Demontis model). Henry coefficients of ethylbenzene significantly vary within MFI-type zeolite structures. For the crystal structures from experiments, the Henry coefficients of ethylbenzene in the Mono and Ortho structure are similar and larger than in the Para structure.

Significant differences can be observed using the modified and original host−host force fields. For the original Demontis[103] model in the Para structure, the Henry coefficient of ethylbenzene is 3.4 times smaller than when taking the equilibrium bond lengths directly from the crystal structure from experiments in the modified Demontis model. This suggests that Henry coefficients (and hence adsorption) of ethylbenzene in MFI-type zeolites are very sensitive to small deviations in the atom positions of the zeolite framework.

3.2. Adsorption of *n*-Heptane in MFI-Type Zeolite. The adsorption of *n*-heptane in MFI Ortho at 303 K is calculated with the modified Nicholas[105] model, the rigid framework with atomic positions fixed to the crystal from experiments,[67] and the rigid framework with atom positions optimized at 0 K using the modified Nicholas[105] model. The adsorption isotherms are shown in Figure 4. Experimental data from Sun et al.[147] is included. The simulation results by Vlugt and Schenk[63] are included. The simulation by Vlugt and Schenk[63] were performed using a modified Demontis-like model, by tuning the spring constants $k/k_B = k_{O-O}/k_B = 0.2k_{Si-O}/k_B$, from 6000 to 100000 KÅ^{-2} (original Demontis[103] model: $k_{O-O}/k_B = 51831.61$ KÅ^{-2}). The simulations using the rigid framework slightly underestimate the amount of adsorbed molecules when the loading is higher than 4 molec./uc. Using the rigid structure with atom positions optimized at
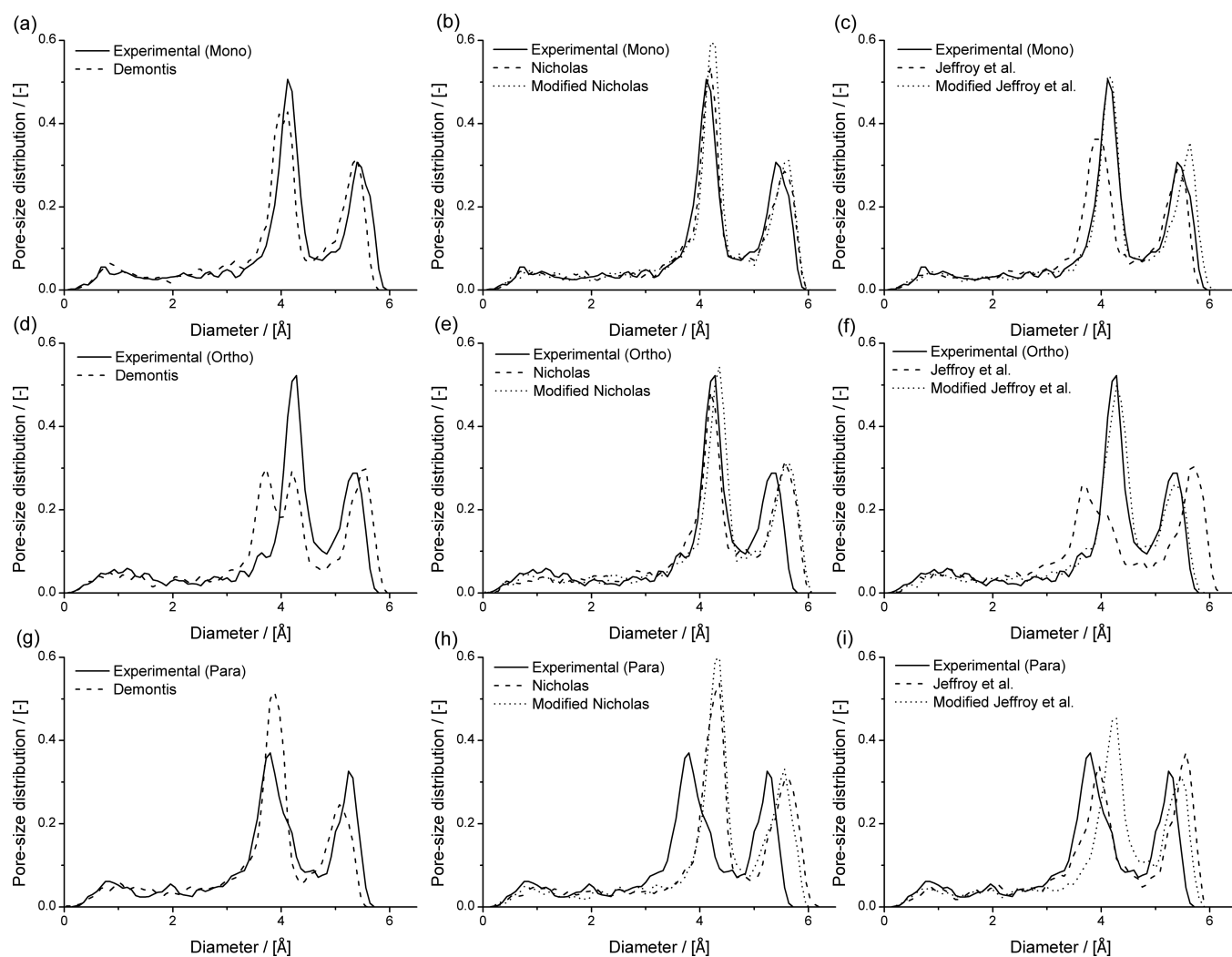
Figure 3. Pore-size distributions (PSDs) of MFI-type zeolite structures optimized at 0 K with the flexible host−host models. Experiments correspond to the PSD computed in lattices from experiments (Mono,[84] Ortho,[67] and Para[28]). PSD of the MFI (a) Mono, (c) Ortho, and (g) Para structures with atom positions optimized at 0 K using the Demontis[103] model. PSD of the MFI (b) Mono, (e) Ortho, and (h) Para structures with atom positions optimized at 0 K using the original and the modified Nicholas[105] model. PSD of the MFI (c) Mono, (f) Ortho, and (i) Para structures with atom positions optimized at 0 K using the original and modified model by Jeffroy et al.[16] In a PSD of MFI-type zeolites, the peak centered at a diameter of approximately 4 Å corresponds to the channels. The peak centered at a diameter of approximately 5.5 Å corresponds to the intersection of the channels.

Table 1. Mean and Maximum Displacement (Å) of the Atomic Positions between the Experimental MFI-Type Structures, the Rigid Structure with Atom Positions Optimized at 0 K Using the Host−Host Force Fields, and the Modified Forms[a]

	Mono			Ortho			Para		
	mean (Å)	max (Å)	$K_{H,eb}$ (mmol/kg Pa)	mean (Å)	max (Å)	$K_{H,eb}$ (mmol/kg Pa)	mean (Å)	max (Å)	$K_{H,eb}$ (mmol/kg Pa)
Demontis[103]	0.211	0.582	14.9(11)	0.282	0.679	13.9(5)	0.315	0.786	3.6(3)
Mod. Demontis[103]	0.000	0.000	24.3(11)	0.000	0.000	26.1(24)	0.000	0.000	12.3(8
Nicholas[105]	0.216	0.511	24.6(13)	0.229	0.497	30.9(15)	0.455	1.081	25.8(9)
Mod. Nicholas[105]	0.164	0.449	30.3(10)	0.189	0.536	44.2(15)	0.342	0.611	31.1(9)
Jeffroy et al.[16]	0.271	0.658	9.8(3)	0.419	1.065	10.8(4)	0.475	1.238	13.2(4)
Mod. Jeffroy et al. 16	0.137	0.311	29.8(13)	0.226	0.656	27.8(20)	0.462	1.109	22.4(11)

[a]$K_{H, eb}$ is the Henry coefficient of ethylbenzene at 353 K in the MFI-type structures with atom positions optimized at 0 K using the host−host force fields and the modified forms. The Henry coefficient of ethylbenzene in the MFI-type structures with atom positions optimized at 0 K using the modified Demontis[103] model correspond to the Henry coefficient in the crystal structure from experiments. The numbers in parentheses denote the statistical uncertainties in the last digit.

0 K using the modified Nicholas model, the experimental loadings are slightly overpredicted. These differences between the loadings in the rigid and the rigid structure with atom

positions optimized at 0 K are related to the pore size changes induced by the modified Nicholas model. The loadings computed using the modified Nicholas model are close to
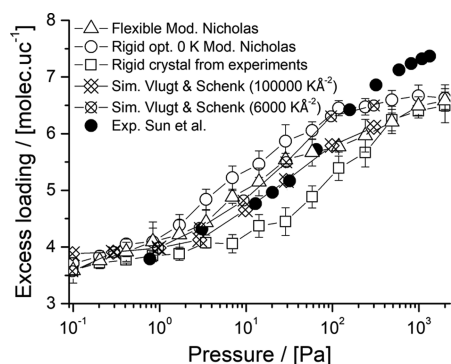
Figure 4. Adsorption isotherm of *n*-heptane in MFI Ortho at 303 K. Experimental data from Sun et al.[147] Closed symbols denote the experimental data. Crossed symbols denote the simulations by Vlugt and Schenk.[63] Open triangles, circles, and squares denote simulations using the modified Nicholas[105] model, the rigid structure with atom positions optimized at 0 K with the modified Nicholas model, and the rigid crystal structure from experiments,[67] respectively.

the experimental loadings. The isotherm computed using the modified Nicholas model is in excellent agreement with the predictions of Vlugt and Schenk.[63] All simulations underestimate the experimental loadings at high pressures. All simulated isotherms converge to the same maximum loading of approximately 6.5 molec./uc. in the studied pressure range. The simulations suggest that there is marginal contribution of the flexibility models in the prediction of *n*-heptane loadings in MFI-type zeolites as the differences are small and below the statistical uncertainties of the simulations.

3.3. Adsorption of Ethylbenzene in MFI-Type Zeolites. Figure 5 shows the adsorption isotherm of
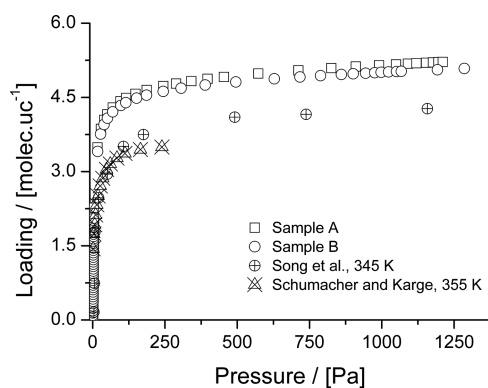

Figure 5. Experimental adsorption isotherm of ethylbenzene in MFI-type zeolite samples (Si/Al ratio: 80) at 353 K. Sample A and B are obtained in this work. Experimental data of ethylbenzene adsorption in MFI-type zeolites by Song et al.[40] at 345 K (Si/Al ratio: 1338) and Schumacher and Karge[35] at 355 K (Si/Al ratio: 34) are included. Experimental data are listed in the Supporting Information.

ethylbenzene in MFI-type zeolites (Si/Al ratio: 80) at 353 K, experimentally obtained in this work. The experimental loadings obtained in this work are listed in the Supporting Information. The adsorption of ethylbenzene in MFI-type zeolites has been reported by Song et al.[40] at 345 K (Si/Al ratio: 1338) and Schumacher and Karge[35] at 355 K (Si/Al ratio: 34). Type I isotherms are reported with a maximum loadings of approximately 4 and 3.5 molec./uc, respectively.

Choudhary and Srinivasan[148] reported the effect of the Si/Al ratio in the adsorption of benzene in MFI-type zeolites at 523 K. It is observed that the loadings of benzene increase with the decrease in the Si/Al ratio. Guo et al.[149] indicate that the pore size of MFI-type zeolites become smaller with increasing Si/Al ratios of the framework. This suggest that the loadings of ethylbenzene from this work are expected to be higher than the loadings reported by Song et al.[40] and lower than the loadings reported by Schumacher and Karge[35] due to differences in the Si/Al ratio of the zeolites. In this work, loadings over 4 molec./uc are observed at pressures higher than 40 Pa. The loadings reached 5 molec./uc at approximately 800 Pa. The maximum loading obtained is 5.21 at 1211 Pa in sample A. The loadings obtained in this work are higher than the loadings reported in the literature.[35,40] This suggest that the differences between the loadings obtained in this work and the isotherms from literature[35,40] are not related to Si/Al ratio differences. The experimental data from this work suggests that the channels of MFI-type zeolites are able to host ethylbenzene molecules when the intersections are loaded at 353 K.

The adsorption of ethylbenzene in MFI-type zeolites at 353 K is calculated using the modified Nicholas model, the modified Demontis model, the rigid experimental lattice, and the rigid framework with atom positions optimized at 0 K with the modified Nicholas model in the Mono, Ortho, and Para MFI-type structures. The adsorption isotherms (Si/Al ratio: ∞) and the experimental data (Si/Al ratio: 80) are shown in Figure 6. Experimental observations reported that the MFI/ethylbenzene system is in the Mono structure when the loading is lower than 4 molec./uc.[26]

All simulations using the modified Demontis model reach approximately 4 molec./uc at the high pressure in the considered pressure range. All the molecules are located in the intersections of the channels.

For the Mono and Ortho structures, framework flexibility using the modified Demontis model does not show any contribution to the loadings compared to the use of the rigid frameworks from crystallography. In the case of the Para structure, the loadings obtained with the modified Demontis model are lower than in the rigid structure at high pressures.

In the Mono structure, the use of the modified Nicholas model does not show any influence of the framework flexibility when the loading is lower than 4 molec./uc compared to the rigid structures. The ethylbenzene loading in the rigid structure with atom positions fixed to the crystal structure from experiments and the rigid structure with atom positions optimized at 0 K both reach 4 molec./uc in the considered pressure range. At 2000 Pa, a loading of approximately 0.5 molec./uc higher than in the rigid frameworks are obtained. At pressures higher than 200 Pa, loadings higher than 4 molec./uc are obtained with the modified Nicholas model. When using the modified Nicholas model, the framework flexibility plays a role when loadings are higher than 4 molec./uc.

In the Ortho structure, the simulations using the modified Nicholas model and the rigid structure with atom positions optimized at 0 K predict higher loadings than in the rigid framework from crystallography. Ethylbenzene loadings reach approximately 4 molec./uc with the rigid frameworks and slightly higher loadings with the modified Nicholas model. In the Para structure, ethylbenzene loadings are similar when using the modified Nicholas model and the rigid structure with atom positions optimized at 0 K for pressures up to 100 Pa. At 2000 Pa, the simulations with the modified Nicholas model
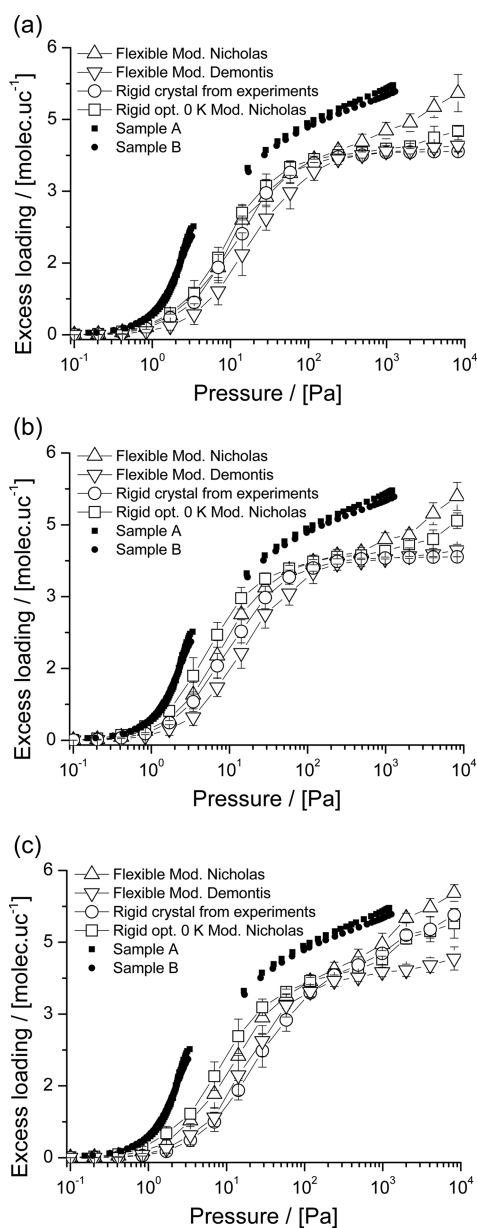
Figure 6. Adsorption isotherms of ethylbenzene at 353 K computed for the (a) Mono, (b) Ortho, and (c) Para structures (Si/Al ratio: ∞). Closed symbols denote the experimental data from this work (Si/Al ratio: 80). Open triangles, upside down triangles, circles, and squares denote the simulations with the modified Nicholas[105] model, the modified Demontis[103] model, the rigid structure with atom positions optimized at 0 K using the modified Nicholas model, and the rigid structure from experiments, respectively.

predict loadings 0.5 molec./uc higher than in the rigid frameworks. At high pressures, the loadings in the rigid and the rigid structure with atom positions optimized at 0 K are the same. A typical snapshot of the simulation of adsorption in MFI Para using the modified Nicholas model at 353 K and 2000 Pa is included in the Supporting Information. It can be observed that ethylbenzene molecules are located in the channels and in the intersections of the channels.

Obtaining higher loadings in the rigid structure with atom positions optimized at 0 K than in the rigid structure from experiments suggests that the atomic configuration of the optimized structure at 0 K can be related to the pore-size

difference shown in Figure 3h. The intersection of the rigid structure with atom positions optimized at 0 K using the modified Nicholas model are approximately 0.5 Å larger than in the rigid crystal structure from experiments.

Comparing the Mono, Ortho, and Para systems, higher maximum loadings are obtained in the Para structure for all cases. The adsorption of molecules in the Mono structure is less affected by use of the modified Nicholas model at low loadings. There is a qualitatively good agreement between the simulations using the modified Nicholas model and the experimental data. For loadings lower than 4 molec./uc, the simulations using the Mono structure are in good agreement with the experiments, and the flexibility does not play a role in this regime. The loadings computed in the MFI Mono rigid structure with atom positions optimized at 0 K are closer to the experimental loadings than with the rigid structure. At loadings higher than 4 molec./uc, the simulations in the Para structure using the modified Nicholas model show a better agreement with the experiments than using the rigid frameworks and the modified Demontis model.

3.4. Adsorption of Xylene Isomers in MFI-Type Zeolites. The adsorption of xylene isomers in MFI-type zeolites at 373 K is calculated with the modified Nicholas model, the modified Demontis model, the rigid framework and the rigid structure with atom positions optimized at 0 K with the modified Nicholas model. The adsorption isotherms are shown in Figures 7, 8, and 9. For *m*-xylene (Figure 7) in the Mono structure, framework flexibility does not influence the isotherm. The differences in the loadings using the modified Nicholas model, the modified Demontis model, the rigid structure from experiments and the rigid structure with atom positions optimized at 0 K are below the statistical error of the simulations. In the Ortho structure, the highest loadings are predicted in the rigid structure with atom positions optimized at 0 K. At 800 Pa, all simulations predict a loading of approximately 4 molec./uc. In the Para structure, the modified Nicholas model and the rigid structure with atom positions optimized at 0 K using the modified Nicholas model predict higher loadings than in the rigid structure from experiments and with the modified Demontis model. This suggests that obtaining higher loadings with the modified Nicholas model is due to the deformation of the crystal structure (in the structure with atom positions optimized at 0 K) instead of the vibrations of atoms. In the *m*-xylene/MFI-type zeolite system, the flexibility of the zeolite does not play a large role in the adsorption. All simulations of adsorption of *m*-xylene in the MFI-type zeolites overestimate the experimental data.

For *o*-xylene (Figure 8), the loadings predicted with the modified Nicholas model and the rigid structure with atom positions optimized at 0 K using the modified Nicholas model are higher than in the rigid structure for each MFI-type zeolite lattice. A very small influence of the flexibility of the modified Nicholas model can be observed for each structure. The computed loadings differ within the statistical error with the rigid structure with atom positions optimized at 0 K using the modified Nicholas model. The loadings obtained with the modified Demontis model are lower than in the rigid structure from experiments.

It is important to note that the loadings from experiments of adsorption in silicalite[36] at 373 K for *m*-xylene are much lower than those reported for *o*-xylene. The loadings reported by Wu et al.[36] at 293 K show higher loadings for *m*-xylene than for *o*-

Figure 7. Adsorption isotherms of *m*-xylene at 373 K computed in the (a) Mono, (b) Ortho, and (c) Para structures. Closed symbols denote the experimental data from Wu et al.[36] Open triangles, upside down triangles, circles, and squares denote the simulations with the modified Nicholas[105] model, the modified Demontis[103] model, the rigid structure with atom positions optimized at 0 K using the modified Nicholas model, and the rigid structure from experiments, respectively.
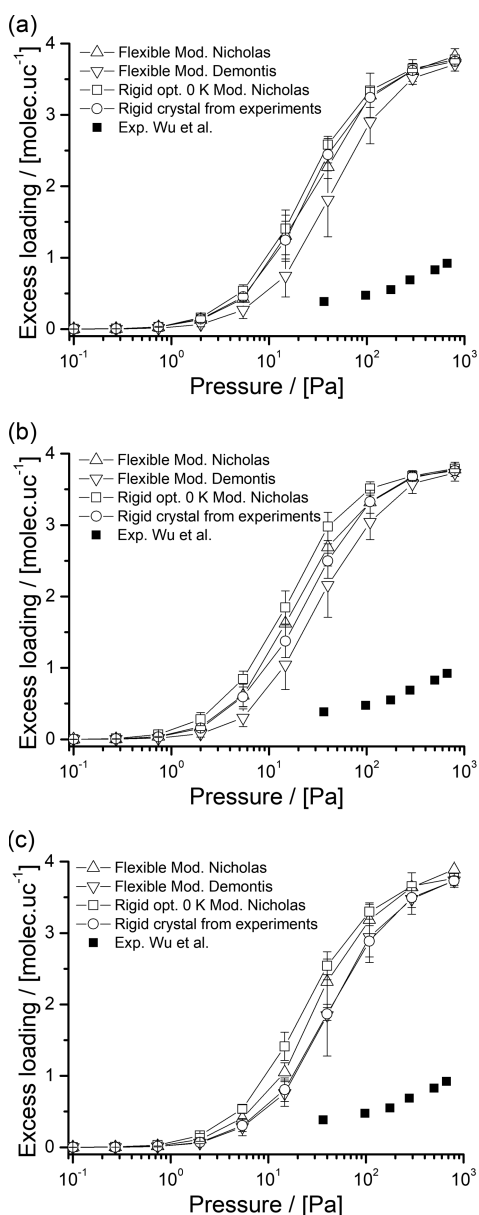

Figure 8. Adsorption isotherms of *o*-xylene at 373 K computed in the (a) Mono, (b) Ortho, and (c) Para structures. Closed symbols denote the experimental data from Wu et al.[36] Open triangles, upside down triangles, circles, and squares denote the simulations with the modified Nicholas[105] model, the modified Demontis[103] model, the rigid structure with atom positions optimized at 0 K using the modified Nicholas model, and the rigid structure from experiments, respectively.

xylene in silicalite. This suggests that the loadings of *m*-xylene at 373 K in silicalite can be hindered by slow diffusion.

The modified Demontis model yields loadings closer to the experimental data than any of the models here considered.

For *p*-xylene (Figure 9) in the Mono and Ortho structures, the modified Nicholas model predicts higher loadings than the rigid structures only at 800 Pa. At lower pressures, the differences are below the statistical uncertainties of the simulations. The modified Demontis model predicts the lowest loadings in all MFI-type zeolite structures. The loadings obtained with the modified Demontis model are lower than in the rigid structure from experiments. The modified Demontis model yields loadings in excellent agreement with the
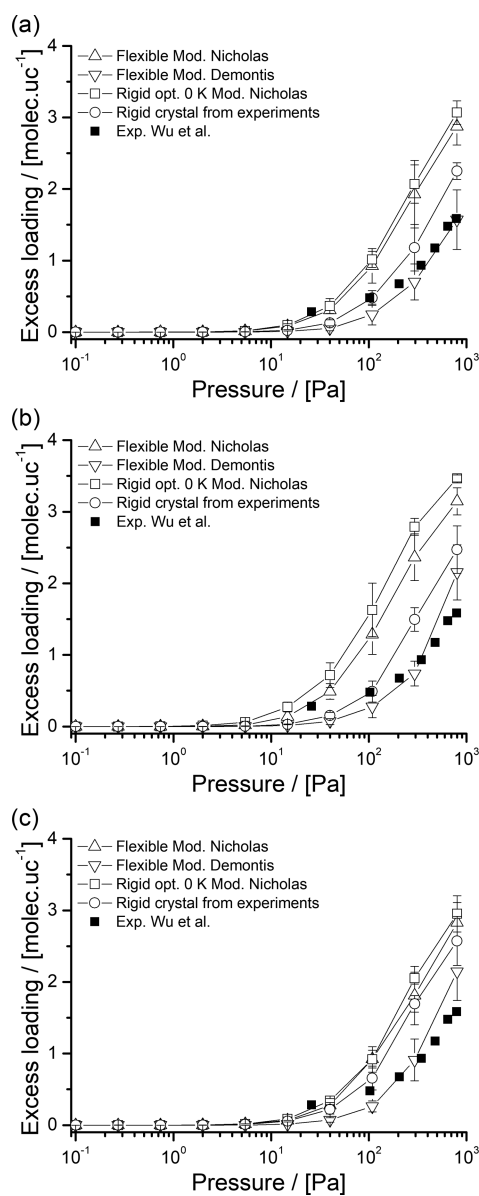
experimental isotherm. In the Para structure, the loadings computed in the rigid structure from experiments are higher than with any flexible model considered. The modified Nicholas model yields loadings close to the rigid structure with atom positions optimized at 0 K, which suggests that the flexibility does not play a role in this case. The large differences between the loadings in the rigid structure from experiments and with the modified Demontis model at high pressures suggests that the adsorption of molecules in the intersections of the Para structure is affected by the displacement of the zeolite atoms.

3.5. Discussion. The simulations from this work underscore the difficulties in modeling the framework flexibility and
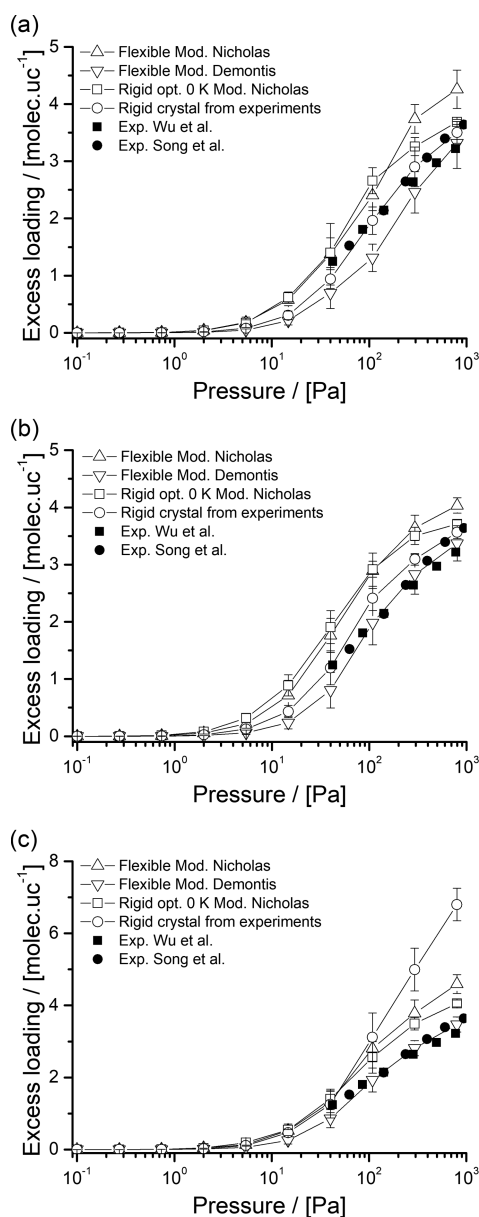
Figure 9. Adsorption isotherms of *p*-xylene at 373 K computed in the (a) Mono, (b) Ortho, and (c) Para structures. Closed circles and squares denote the experimental data from Wu et al.[36] and Song et al.,[40] respectively. Open triangles, upside down triangles, circles, and squares denote the simulations with the modified Nicholas[105] model, the modified Demontis[103] model, the rigid structure with atom positions optimized at 0 K using the modified Nicholas model, and the rigid structure from experiments, respectively.

The simulations show that the long-range potentials (intraframework electrostatic and Lennard-Jones interactions) in flexible framework models intrinsically induce small but important changes in the atom positions of the zeolite and hence in the adsorption isotherms. The incompatibility of the partial charges of the zeolite atoms between host−host and guest−host interactions shows the need to consider both aspects for force fields development.

The adsorption of alkylbenzenes in the pores of MFI-type zeolites represents confinement conditions. The confinement affects the physico-chemistry of the adsorbed molecules in different aspects.[150,151] The confinement optimizes van der Waals interactions in zeolite cavities, involving a perturbation of the shape and electronic structure of the sorbate.[25] This suggests that polarizability of sorbate molecules as well as the zeolite framework might have been overlooked.

Macroscopic behavior and properties of alkylbenzenes, such as VLE and critical points, can be well predicted with models that consider rigid molecules in gas and liquid phases.[131] However, benzene rings are flexible.[152] Laaksonen et al.[153] reported that isolated benzene molecules can easily adopt non-planar conformations with torsion angles up to 10° at room temperature. Considering a C−C bond length of 1.4 Å, a C−C−C−C torsion angle of 10° in the aromatic ring induces a displacement of a C atom of approximately 0.24 Å. Such displacement is similar to the mean displacement of the zeolite atoms induced by the force fields for framework flexibility discussed in this work (see Table 1). This suggests that the intramolecular flexibility of aromatic molecules can be an important factor in the description of adsorption of aromatics in a zeolite pore.

Experimental work highlights challenges for an accurate description of the adsorption process. Data of adsorption of aromatics in MFI-type zeolites is scarce and not always consistent under the same temperature/pressure conditions. The experiments presented in this work show important differences with experiments from the literature performed decades ago. This suggests that experiments of adsorption of aromatics in MFI-type zeolites are highly dependent on the sample synthesis and detection methods. Such inconsistencies can also be related to diffusion limitations experienced by aromatic bulky molecules, such as *m*-xylene and *o*-xylene.[154,155] The differences between experiments of adsorption of aromatics in MFI-type zeolites does not provide a clear overview on what to compare with simulations results, what to fit, or what to use as input for machine learning algorithms for force field development.

An accurate experimental description of the internal changes and crystal structure of the zeolite when varying pressure or temperature is needed. To the best of authors' knowledge, detailed experimental insights on how the crystal structure changes hosting different aromatic molecules are not available. All this information is required to develop models able to reproduce and provide reliable molecular insights about the adsorption phenomena. Such requirements, pitfalls, and challenges underline that adsorption of aromatics in MFI-type zeolites is one of the most difficult systems to model.

4. CONCLUSIONS

The adsorption of *n*-heptane, ethylbenzene, and xylene isomers in MFI-type zeolites is computed using rigid and flexible zeolite frameworks. New experimental data of the adsorption of ethylbenzene in a MFI-type zeolite at 353 K is presented.

the adsorption of aromatics in MFI-type zeolites appropriately. Models able to describe the phase transitions that MFI-type zeolites show in experiments such as core−shell are difficult to combine with adsorbate models to study adsorption.[74] Also, the use of a core−shell model implies a significant increase in the number of particles in the system, which reduces the efficiency of the simulation.[74] For modeling the phase transitions of MFI-type zeolites, the small volume change and shape differences between the phases cannot be accounted assuming a fixed unit cell volume. Systems where adsorbed molecules induce rearrangement of the zeolite pores require host−host force fields specially designed for this purpose.

The experimental data shows significantly higher loadings than previously reported isotherms from the literature. Pore-size distributions (PSDs) of the MFI-type zeolite structures subject to three different host–host force field are computed. The PSDs show that the use of constant bond lengths induces displacements of the framework atoms that influence adsorption. Directly taking the bond lengths from the crystallographic structure minimizes this effect. The electrostatic and LJ intraframework interactions induce displacements of the zeolite atoms that significantly affect the size of the pores and channels of the zeolite. The simulations of the adsorption of *n*-heptane in MFI-type zeolite at 303 K show a minor influence of framework flexibility for the computed isotherms compared to simulations using the rigid frameworks and experimental data. The simulations of adsorption of ethylbenzene in MFI-type zeolite at 353 K show that the simulations with the modified Demontis model underestimate experimental loadings. The results suggest that the framework atom displacements using the modified Demontis model hinder the adsorption of aromatics in the zeolite. The use of the modified Nicholas model yields loadings closer to the experimental data. This is due to changes in the average zeolite structure caused by the intraframework interactions and not to framework flexibility. The vibrations of the zeolite atoms using the modified Nicholas model in the adsorption of ethylbenzene in MFI-type zeolites only play a role at high pressures/loadings.

The simulations of adsorption of xylene isomers in MFI-type zeolites at 373 K showed that the influence of the flexibility is dependent on the framework. The use of the rigid framework and the modified Demontis model yields loadings close to the experimental isotherm for *o*-xylene and *p*-xylene. All simulations overestimate the experimental isotherm of *m*-xylene. *p*-Xylene in the Para structure is the only case where the flexible models show significantly lower loadings than in the rigid structure from experiments. The loadings in the rigid structure are higher than with framework flexibility models and overestimate the experimental loadings.

Using the considered host–host force fields, framework flexibility generates a new structure that is differently "rigid". The flexible force fields produce a zeolite structure that vibrates around a new equilibrium configuration that has limited capacity to accommodate to a bulky guest molecule. The vibration of the zeolite atoms only plays role at high loadings, and the adsorption is mainly dependent on the average positions of the atoms. The intraframework interactions should be treated carefully as these interactions cause significant deviations from the experimental zeolite lattice. The adsorption of *n*-heptane in the MFI-type zeolite is not significantly influenced by the structure changes of the framework due to the force fields for framework flexibility (see Figure 4). The use of a zeolite structure with fixed atom positions is appropriate when the molecule does not fit tightly in the zeolite pores. For aromatics, the influence of the force field for framework flexibility on the adsorption in MFI-type zeolites implies that the structural changes of the zeolite framework are relevant for molecules that fit tightly in the zeolite void spaces. The prediction of different loadings when a force field for framework flexibility is used compared to when a rigid structure is used is an artifact of the force field and not a re-accommodation of the framework atoms to a guest molecule. Force fields for framework flexibility usually do not capture the physics behind the accommodation of the framework atoms to a guest molecule. Obtaining a prediction of the loadings closer to the experiments is an overall effect of the host–host interactions and not guest interactions as desired. This implies that it is not possible to determine if one of the force fields for framework flexibility performs best for the description of the adsorption of aromatics in MFI-type zeolites. Simulations of MOFs and other porous material considering framework flexibility use similar types of force fields.[72,74] The findings of this work suggest that similar effects on the framework may be found for other classes of porous materials. The intraframework interactions of the modified Demontis model do not intrinsically change the zeolite structure. Using different spring constants in such a model could be of interest to investigate if the zeolite framework atoms can rearrange to accommodate guest molecules.

The simulations underline the need of new tailor-made force fields to model the zeolite flexibility for aromatics. Such force fields should focus on the local changes due to the presence of bulky guest molecules and not only vibrational behavior. As electrostatic interactions are important for adsorption purposes, the intraframework LJ interactions should also aim to balance the electrostatic interactions to preserve the atomic positions of the zeolite. There are many challenges and difficulties to model the framework flexibility and the adsorption of aromatics in MFI-type zeolites appropriately. An accurate experimental description of the internal changes and crystal structure of the zeolite when varying pressure or temperature is crucial. Data of adsorption of aromatics in MFI-type zeolites is scarce and not always consistent at the same temperature/pressure conditions. The variability on the experiments of adsorption of aromatics in MFI-type zeolites does not provide a clear overview on what to compare to the predictions of the simulations. This knowledge is required to develop models able to reproduce and provide reliable molecular insights about the adsorption phenomena. The simulations from this work show that force fields for framework flexibility should not be blindly applied to zeolites, and a general rethinking of the parametrization schemes for such models is needed.

ASSOCIATED CONTENT

Ⓢ Supporting Information

The Supporting Information is available free of charge at https://pubs.acs.org/doi/10.1021/acs.jpcc.0c06096.

> The crystal structures of MFI-type zeolites with atom positions optimized at 0 K using the Demontis[103] model, the Nicholas[105] model, and the model by Jeffroy et al.[16] in CIF format (ZIP)

> The parameters of the force fields used in this work, a typical snapshot of the simulation of adsorption of ethylbenzene in MFI Para using the modified Nicholas model at 353 K and 2000 Pa, and the experimental loadings of ethylbenzene in Samples A and B of MFI-type zeolite at 353 K (PDF)

AUTHOR INFORMATION

Corresponding Author

Thijs J. H. Vlugt − *Engineering Thermodynamics, Process & Energy Department, Faculty of Mechanical, Maritime and Materials Engineering, Delft University of Technology, 2628 CB Delft, The Netherlands;* ⓞ orcid.org/0000-0003-3059-8712; Email: t.j.h.vlugt@tudelft.nl

Authors

Sebastián Caro-Ortiz − *Engineering Thermodynamics, Process & Energy Department, Faculty of Mechanical, Maritime and Materials Engineering, Delft University of Technology, 2628 CB Delft, The Netherlands*

Erik Zuidema − *Shell Global Solutions International B.V., 1030 BN Amsterdam, The Netherlands*

Desmond Dekker − *Shell Global Solutions International B.V., 1030 BN Amsterdam, The Netherlands*

Marcello Rigutto − *Shell Global Solutions International B.V., 1030 BN Amsterdam, The Netherlands*

David Dubbeldam − *Van 't Hoff Institute of Molecular Sciences, University of Amsterdam, 1098 XH Amsterdam, The Netherlands;* orcid.org/0000-0002-4382-1509

Complete contact information is available at:
https://pubs.acs.org/10.1021/acs.jpcc.0c06096

Notes

The authors declare no competing financial interest.

■ REFERENCES

(1) Princz, P.; Olah, J.; Smith, S.; Hatfield, K.; Litrico, M. In *Use of humic substances to remediate polluted environments: From theory to practice; Perminova, I. V.* Hatfield, K., Hertkorn, N., Eds.; *Springer Netherlands*, 2005; pp. 267−282.

(2) Milán, Z.; de Las Pozas, C.; Cruz, M.; Borja, R.; Sánchez, E.; Ilangovan, K.; Espinosa, Y.; Luna, B. The removal of bateria by modified natural zeolites. *J. Environ. Sci. Health A* **2001**, *36*, 1073−1087.

(3) Primo, A.; Garcia, H. Zeolites as catalysts in oil refining. *Chem. Soc. Rev.* **2014**, *43*, 7548−7561.

(4) Borai, E. H.; Harjula, R.; Malinen, L.; Paajanen, A. Efficient removal of cesium from low-level radioactive liquid waste using natural and impregnated zeolite minerals. *J. Hazard. Mater.* **2009**, *172*, 416−422.

(5) Valdés, H.; Alejandro, S.; Zaror, C. A. Natural zeolite reactivity towards ozone: The role of compensating cations. *J. Hazard. Mater.* **2012**, *227-228*, 34−40.

(6) Van Speybroeck, V.; Hemelsoet, K.; Joos, L.; Waroquier, M.; Bell, R. G.; Catlow, C. R. A. Advances in theory and their application within the field of zeolite chemistry. *Chem. Soc. Rev.* **2015**, *44*, 7044−7111.

(7) Kubů, M.; Millini, R.; Žilková, N. 10-ring Zeolites: Synthesis, characterization and catalytic applications. *Catal. Today* **2019**, *324*, 3−14.

(8) Jiang, N.; Erdős, M.; Moultos, O. A.; Shang, R.; Vlugt, T. J. H.; Heijman, S. G. J.; Rietveld, L. C. The adsorption mechanisms of organic micropollutants on high-silica zeolites causing S-shaped adsorption isotherms: An experimental and Monte Carlo simulation study. *Chem. Eng. J.* **2020**, *389*, 123968.

(9) Kulprathipanja, S., Ed. *Zeolites in industrial separation and catalysis*, 1st ed.; John Wiley & Sons, Ltd, 2010.

(10) Smit, B.; Maesen, T. L. M. Molecular simulations of zeolites: Adsorption, diffusion, and shape selectivity. *Chem. Rev.* **2008**, *108*, 4125−4184.

(11) Vlugt, T. J. H.; Zhu, W.; Kapteijn, F.; Moulijn, J. A.; Smit, B.; Krishna, R. Adsorption of linear and branched alkanes in the zeolite silicalite-1. *J. Am. Chem. Soc.* **1998**, *120*, 5599−5600.

(12) Sweeney, W. A.; Bryan, P. F. BTX processing; *Kirk-Othmer Encyclopedia of Chemical Technology; American Cancer Society*, 2000.

(13) Bellussi, G. In *Recent advances in the science and technology of zeolites and related materials*; van Steen, E., Claeys, I., Callanan, L., Eds.; Studies in surface science and catalysis; Science Direct, 2004; Vol. *154*; pp. 53−65.

(14) Ali, S. A.; Aitani, A. M.; Čejka, J.; Al-Khattaf, S. S. Selective production of xylenes from alkyl-aromatics and heavy reformates over dual-zeolite catalyst. *Catal. Today* **2015**, *243*, 118−127.

(15) Gołąbek, K.; Tarach, K. A.; Góra-Marek, K. Xylenes transformation over zeolites ZSM-5 ruled by acidic properties. *Spectrochim. Acta A* **2018**, *192*, 361−367.

(16) Jeffroy, M.; Nieto-Draghi, C.; Boutin, A. Molecular simulation of zeolite flexibility. *Mol. Simulat.* **2014**, *40*, 6−15.

(17) Sartbaeva, A.; Wells, S. A.; Treacy, M. M. J.; Thorpe, M. F. The flexibility window in zeolites. *Nat. Mater.* **2006**, *5*, 962−965.

(18) Poursaeidesfahani, A.; Torres-Knoop, A.; Rigutto, M.; Nair, N.; Dubbeldam, D.; Vlugt, T. J. H. Computation of the heat and entropy of adsorption in proximity of inflection points. *J. Phys. Chem. C* **2016**, *120*, 1727−1738.

(19) Smit, B.; Maesen, T. L. M. Commensurate 'freezing' of alkanes in the channels of a zeolite. *Nature* **1995**, *374*, 42−44.

(20) Talu, O.; Guo, C. J.; Hayhurst, D. T. Heterogeneous adsorption equilibria with comparable molecule and pore sizes. *J. Phys. Chem.* **1989**, *93*, 7294−7298.

(21) Floquet, N.; Coulomb, J. P.; Weber, G.; Bertrand, O.; Bellat, J. P. Structural signatures of type IV isotherm steps: Sorption of trichloroethene, tetrachloroethene, and benzene in silicalite-I. *J. Phys. Chem. B* **2003**, *107*, 685−693.

(22) Fyfe, C. A.; Strobl, H.; Kokotailo, G. T.; Kennedy, G. J.; Barlow, G. E. Ultrahigh-resolution silicon-29 solid-state MAS NMR investigation of sorbate and temperature-induced changes in the lattice structure of zeolite ZSM-5. *J. Am. Chem. Soc.* **1988**, *110*, 3373−3380.

(23) de Vos Burchart, E.; van Bekkum, H.; van de Graaf, B. Molecular mechanics studies on MFI-type zeolites: Part 3. The monoclinic-orthorhombic phase transition. *Zeolites* **1993**, *13*, 212−215.

(24) Ilić, B.; Wettstein, S. G. A review of adsorbate and temperature-induced zeolite framework flexibility. *Microporous Mesoporous Mater.* **2017**, *239*, 221−234.

(25) Pera-Titus, M. Thermodynamic analysis of type VI adsorption isotherms in MFI zeolites. *J. Phys. Chem. C* **2011**, *115*, 3346−3357.

(26) Lee, C.-K.; Chiang, A. S. T. Adsorption of aromatic compounds in large MFI zeolite crystals. *J. Chem. Soc., Faraday Trans.* **1996**, *92*, 3445−3451.

(27) Song, L.; Rees, L. V. C. Adsorption and diffusion of cyclic hydrocarbon in MFI-type zeolites studied by gravimetric and frequency-response techniques. *Microporous Mesoporous Mater.* **2000**, *35-36*, 301−314.

(28) van Koningsveld, H.; Tuinstra, F.; van Bekkum, H.; Jansen, J. C. The location of p-xylene in a single crystal of zeolite H-ZSM-5 with a new, sorbate-induced, orthorhombic framework symmetry. *Acta Crystallogr. B* **1989**, *45*, 423−431.

(29) Daramola, M. O.; Burger, A. J.; Pera-Titus, M.; Giroir-Fendler, A.; Miachon, S.; Dalmon, J.-A.; Lorenzen, L. Separation and isomerization of xylenes using zeolite membranes: a short overview. *Asia-Pac. J. Chem. Eng.* **2010**, *5*, 815−837.

(30) Sacerdote, M.; Bosselet, F.; Mentzen, B. F. The MFI(ZSM-5)/sorbate systems. Comparison between structural, theoretical and calorimetric results. Part II - The MFI/benzene system. *Mater. Res. Bull.* **1990**, *25*, 593−599.

(31) Sorenson, S. G.; Smyth, J. R.; Kocirik, M.; Zikanova, A.; Noble, R. D.; Falconer, J. L. Adsorbate-induced expansion of silicalite-1 crystals. *Ind. Eng. Chem. Res.* **2008**, *47*, 9611−9616.

(32) Nair, S.; Tsapatsis, M. The location of *o*- and *m*-xylene in silicalite by powder X-ray diffraction. *J. Phys. Chem. B* **2000**, *104*, 8982−8988.

(33) Fyfe, C. A.; Lee, J. S. J. Solid-state NMR determination of the zeolite ZSM-5/ortho-xylene host-guest crystal structure. *J. Phys. Chem. C* **2008**, *112*, 500−513.

(34) Mentzen, B. F.; Lefebvre, F. Flexibility of the MFI silicalite framework upon benzene adsorption at higher pore-fillings: A study by X-ray power diffraction, NMR and molecular mechanics. *Mater. Res. Bull.* **1997**, *32*, 813−820.

(35) Schumacher, R.; Karge, H. G. Sorption and sorption kinetics of ethylbenzene in MFI-Type zeolites studied by a barometric technique. *Collect. Czech. Chem. Commun.* **1999**, *64*, 483−494.

(36) Wu, P.; Debebe, A.; Ma, Y. H. Adsorption and diffusion of C_6 and C_8 hydrocarbons in silicalite. *Zeolites* **1983**, *3*, 118−122.

(37) Cartarius, R.; Vogel, H.; Dembowski, J. Investigation of sorption and intracrystalline diffusion of benzene and toluene on silicalite-1. *Ber. Bunsenges. Phys. Chem.* **1997**, *101*, 193−199.

(38) Hill, S. G.; Seddon, D. Comparison of the sorption of benzene in ZSM-5, silicalite-1, and silicalite-2. *Zeolites* **1991**, *11*, 699−704.

(39) Malović, D.; Vučelić, D. Application of thermal analysis for explaining the sorption of benzene and n-hexane on silicalite. *J. Therm. Anal. Calorim.* **1998**, *53*, 835−842.

(40) Song, L.; Sun, Z.; Duan, L.; Gui, J.; McDougall, G. S. Adsorption and diffusion properties of hydrocarbons in zeolites. *Microporous Mesoporous Mater.* **2007**, *104*, 115−128.

(41) Richards, R. E.; Rees, L. V. C. The sorption of p-xylene in ZSM-5. *Zeolites* **1988**, *8*, 35−39.

(42) Ban, H.; Gui, J.; Duan, L.; Zhang, X.; Song, L.; Sun, Z. Sorption of hydrocarbons in silicalite-1 studied by intelligent gravimetry. *Fluid Phase Equilibr.* **2005**, *232*, 149−158.

(43) Thamm, H. Calorimetric study on the state of aromatic molecules sorbed on silicalite. *J. Phys. Chem.* **1987**, *91*, 8−11.

(44) Rudziński, W.; Narkiewicz-Michałek, J.; Szabelski, P.; Chiang, A. S. T. Adsorption of aromatics in zeolites ZSM-5: A thermodynamic-calorimetric study based on the model of adsorption on heterogeneous adsorption sites. *Langmuir* **1997**, *13*, 1095−1103.

(45) Rodeghero, E.; Chenet, T.; Martucci, A.; Ardit, M.; Sarti, E.; Pasti, L. Selective adsorption of toluene and n-hexane binary mixture from aqueous solution on zeolite ZSM-5: Evaluation of competitive behavior between aliphatic and aromatic compounds. *Catal. Today* **2019**, *345*, 157−164.

(46) Calero, S. In *Modeling of transport and accessibility in zeolites*; Cejka, J., Corma, A., Zones, S., Eds.; Zeolites and Catalysis; *John Wiley & Sons, Ltd*, 2010; pp. 335−360.

(47) Fang, H.; Demir, H.; Kamakoti, P.; Sholl, D. S. Recent developments in first-principles force fields for molecules in nanoporous materials. *J. Mater. Chem. A* **2014**, *2*, 274−291.

(48) Ungerer, P.; Tavitian, B.; Boutin, A. *Applications of molecular simulation in the oil and gas industry - Monte-Carlo methods*, 1st ed.; Editions Technip, 2005.

(49) Snurr, R. Q.; Bell, A. T.; Theodorou, D. N. Prediction of adsorption of aromatic hydrocarbons in silicalite from grand canonical Monte Carlo simulations with biased insertions. *J. Phys. Chem.* **1993**, *97*, 13742−13752.

(50) Li, J.; Talu, O. Structural effect on molecular simulations of tight-pore systems. *J. Chem. Soc., Faraday Trans.* **1993**, *89*, 1683−1687.

(51) Torres-Knoop, A.; Heinen, J.; Krishna, R.; Dubbeldam, D. Entropic separation of styrene/ethylbenzene mixtures by exploitation of subtle differences in molecular configurations in ordered crystalline nanoporous adsorbents. *Langmuir* **2015**, *31*, 3771−3778.

(52) Mohanty, S.; Davis, H. T.; McCormick, A. V. Shape selective adsorption in atomistic nanopores - a study of xylene isomers in silicalite. *Chem. Eng. Sci.* **2000**, *55*, 2779−2792.

(53) Chempath, S.; Snurr, R. Q.; Low, J. J. Molecular modeling of binary liquid-phase adsorption of aromatics in silicalite. *AIChE J.* **2004**, *50*, 463−469.

(54) Sánchez-Gil, V.; Noya, E. G.; Sanz, A.; Khatib, S. J.; Guil, J. M.; Lomba, E.; Marguta, R.; Valencia, S. Experimental and simulation studies of the stepped adsorption of toluene on pure-silica MEL zeolite. *J. Phys. Chem. C* **2016**, *120*, 8640−8652.

(55) Zeng, Y.; Moghadam, P. Z.; Snurr, R. Q. Pore size dependence of adsorption and separation of thiophene/benzene mixtures in zeolites. *J. Phys. Chem. C* **2015**, *119*, 15263−15273.

(56) Yue, X.; Yang, X. Molecular simulation study of adsorption and diffusion on silicalite for a benzene/CO_2 mixture. *Langmuir* **2006**, *22*, 3138−3147.

(57) Zeng, Y.; Ju, S.; Xing, W.; Chen, C. Computer simulation of the adsorption of thiophene/benzene mixtures on MFI and MOR. *Sep. Purif. Technol.* **2007**, *55*, 82−90.

(58) Ban, S.; van Laak, A.; de Jongh, P. E.; van der Eerden, J. P. J. M.; Vlugt, T. J. H. Adsorption selectivity of benzene/propene mixtures for various zeolites. *J. Phys. Chem. C* **2007**, *111*, 17241−17248.

(59) Cosoli, P.; Fermeglia, M.; Ferrone, M. GCMC simulations in zeolite MFI and activated carbon for benzene removal from exhaust gaseous streams. *Mol. Simulat.* **2008**, *34*, 1321−1327.

(60) Jeffroy, M.; Fuchs, A. H.; Boutin, A. Structural changes in nanoporous solids due to fluid adsorption: thermodynamic analysis and Monte Carlo simulations. *Chem. Commun.* **2008**, 3275−3277.

(61) Krishna, R.; van Baten, J. M. Influence of adsorption thermodynamics on guest diffusivities in nanoporous crystalline materials. *Phys. Chem. Chem. Phys.* **2013**, *15*, 7994−8016.

(62) Boulet, P.; Narasimhan, L.; Berg'e-Lefranc, D.; Kuchta, B.; Schäf, O.; Denoyel, R. Adsorption into the MFI zeolite of aromatic molecule of biological relevance. Investigations by Monte Carlo simulations. *J. Mol. Model.* **2009**, *15*, 573−579.

(63) Vlugt, T. J. H.; Schenk, M. Influence of framework flexibility on the adsorption properties of hydrocarbons in the zeolite silicalite. *J. Phys. Chem. B* **2002**, *106*, 12757−12763.

(64) Fuchs, A. H.; Cheetham, A. K. Adsorption of guest molecules in zeolitic materials: Computational aspects. *J. Phys. Chem. B* **2001**, *105*, 7375−7383.

(65) Clark, L. A.; Snurr, R. Q. Adsorption isotherm sensitivity to small changes in zeolite structure. *Chem. Phys. Lett.* **1999**, *308*, 155−159.

(66) Olson, D. H.; Kokotailo, G. T.; Lawton, S. L.; Meier, W. M. Crystal structure and structure-related properties of ZSM-5. *J. Phys. Chem.* **1981**, *85*, 2238−2243.

(67) van Koningsveld, H.; van Bekkum, H.; Jansen, J. C. On the location and disorder of the tetrapropylammonium (TPA) ion in zeolite ZSM-5 with improved framework accuracy. *Acta Crystallogr. B* **1987**, *43*, 127−132.

(68) Castillo, J. M.; Dubbeldam, D.; Vlugt, T. J. H.; Smit, B.; Calero, S. Evaluation of various water models for simulation of adsorption in hydrophobic zeolites. *Mol. Simulat.* **2009**, *35*, 1067−1076.

(69) García-Pérez, E.; Parra, J. B.; Ania, C. O.; Dubbeldam, D.; Vlugt, T. J. H.; Castillo, J. M.; Merkling, P. J.; Calero, S. Unraveling the argon adsorption processes in MFI-Type zeolite. *J. Phys. Chem. C* **2008**, *112*, 9976−9979.

(70) Sánchez-Gil, V.; Noya, E. G.; Guil, J. M.; Lomba, E.; Valencia, S. Adsorption of argon on pure silica MEL Volumetric experiments and grand canonical Monte Carlo simulations. *Microporous Mesoporous Mater.* **2016**, *222*, 218−225.

(71) García-Sánchez, A.; Dubbeldam, D.; Calero, S. Modeling adsorption and self-diffusion of methane in LTA zeolites: The influence of framework flexibility. *J. Phys. Chem. C* **2010**, *114*, 15068−15074.

(72) Fang, H.; Findley, J.; Muraro, G.; Ravikovitch, P. I.; Sholl, D. S. A Strong Test of Atomically Detailed Models of Molecular Adsorption in Zeolites Using Multilaboratory Experimental Data for CO_2 Adsorption in Ammonium ZSM-5. *J. Phys. Chem. Lett.* **2020**, *11*, 471−477.

(73) Schenk, M.; Smit, B.; Maesen, T. L. M.; Vlugt, T. J. H. Molecular simulations of the adsorption of cycloalkanes in MFI-type silica. *Phys. Chem. Chem. Phys.* **2005**, *7*, 2622−2628.

(74) Dubbeldam, D.; Walton, K. S.; Vlugt, T. J. H.; Calero, S. Design, parameterization, and implementation of atomic force fields for adsorption in nanoporous materials. *Adv. Theory Simul.* **2019**, *2*, 1900135.

(75) Park, J.; Agrawal, M.; Gallis, D. F. S.; Harvey, J. A.; Greathouse, J. A.; Sholl, D. S. Impact of intrinsic framework flexibility for selective adsorption of sarin in non-aqueous solvents using metal-organic frameworks. *Phys. Chem. Chem. Phys.* **2020**, *22*, 6441−6448.

(76) Kupgan, G.; Demidov, A. G.; Colina, C. M. Plasticization behavior in polymers of intrinsic microporosity (PIM-1): A simulation study from combined Monte Carlo and Molecular Dynamics. *J. Membrane Sci.* **2018**, *565*, 95−103.

(77) Rogge, S. M. J.; Goeminne, R.; Demuynck, R.; Gutiérrez-Sevillano, J. J.; Vandenbrande, S.; Vanduyfhuys, L.; Waroquier, M.; Verstraelen, T.; Van Speybroeck, V. Modeling gas adsorption in flexible Metal-Organic Frameworks via Hybrid Monte Carlo/Molecular Dynamics schemes. *Adv. Theory Simul.* **2019**, *2*, 1800177.

(78) Chokbunpiam, T.; Fritzsche, S.; Caro, J.; Chmelik, C.; Janke, W.; Hannongbua, S. Importance of ZIF-90 lattice flexibility on diffusion, permeation, and lattice structure for an adsorbed H_2/CH_4 gas mixture: A re-examination by Gibbs ensemble Monte Carlo and Molecular Dynamics simulations. *J. Phys. Chem. C* **2017**, *121*, 10455−10462.

(79) Hajek, J.; Caratelli, C.; Demuynck, R.; De Wispelaere, K.; Vanduyfhuys, L.; Waroquier, M.; Van Speybroeck, V. On the intrinsic dynamic nature of the rigid UiO-66 metal-organic framework. *Chem. Sci.* **2018**, *9*, 2723−2732.

(80) Namsani, S.; Ozcan, A.; Yazaydin, A. Ö. Direct simulation of ternary mixture separation in a ZIF-8 membrane at molecular scale. *Adv. Theory Simul.* **2019**, *2*, 1900120.

(81) Witman, M.; Ling, S.; Jawahery, S.; Boyd, P. G.; Haranczyk, M.; Slater, B.; Smit, B. The influence of intrinsic framework flexibility on adsorption in nanoporous materials. *J. Am. Chem. Soc.* **2017**, *139*, 5547−5557.

(82) Agrawal, M.; Sholl, D. S. Effects of intrinsic flexibility on adsorption properties of Metal-Organic Frameworks at dilute and nondilute loadings. *ACS Appl. Mater. Interfaces* **2019**, *11*, 31060−31068.

(83) Heinen, J.; Dubbeldam, D. On flexible force fields for metal-organic frameworks: Recent developments and future prospects. *WIREs Comput. Mol. Sci.* **2018**, *8*, No. e1363.

(84) van Koningsveld, H.; Jansen, J. C.; van Bekkum, H. The monoclinic framework structure of zeolite H-ZSM-5. Comparison with the orthorhombic framework of as-synthesized ZSM-5. *Zeolites* **1990**, *10*, 235−242.

(85) Sławek, A.; Vicent-Luna, J. M.; Marszałek, B.; Balestra, S. R. G.; Makowski, W.; Calero, S. Adsorption of n-alkanes in MFI and MEL: Quasi-equilibrated thermodesorption combined with molecular simulations. *J. Phys. Chem. C* **2016**, *120*, 25338−25350.

(86) Schwarz, S.; Kojima, M.; O'Connor, C. T. Effect of tetraalkylammonium, alcohol and amine templates on the synthesis and high pressure propene oligomerisation activity of ZSM-type zeolites. *Appl. Catal.* **1991**, *73*, 313−330.

(87) Poursaeidesfahani, A.; Torres-Knoop, A.; Dubbeldam, D.; Vlugt, T. J. H. Direct free energy calculation in the Continuous Fractional Component Gibbs ensemble. *J. Chem. Theory Comput.* **2016**, *12*, 1481−1490.

(88) Shi, W.; Maginn, E. J. Continuous Fractional Component Monte Carlo: An adaptive biasing method for open system atomistic simulations. *J. Chem. Theory Comput.* **2007**, *3*, 1451−1463.

(89) Dubbeldam, D.; Calero, S.; Ellis, D. E.; Snurr, R. Q. RASPA: molecular simulation software for adsorption and diffusion in flexible nanoporous materials. *Mol. Simul.* **2016**, *42*, 81−101.

(90) Dubbeldam, D.; Torres-Knoop, A.; Walton, K. S. On the inner workings of Monte Carlo codes. *Mol. Simul.* **2013**, *39*, 1253−1292.

(91) Dubbeldam, D.; Calero, S.; Vlugt, T. J. H. iRASPA: GPU-accelerated visualization software for materials scientists. *Mol. Simul.* **2018**, *44*, 653−676.

(92) Allen, M. P.; Tildesley, D. J. *Computer simulation of liquids*; 2nd ed.; Oxford University Press: 2017.

(93) Jablonka, K. M.; Ongari, D.; Smit, B. Applicability of tail corrections in the molecular simulations of porous materials. *J. Chem. Theory Comput.* **2019**, *15*, 5635−5641.

(94) Ewald, P. P. Die Berechnung optischer und elektrostatischer Gitterpotentiale. *Ann. Phys.* **1921**, *369*, 253−287.

(95) Torres-Knoop, A.; Balaji, S. P.; Vlugt, T. J. H.; Dubbeldam, D. A comparison of advanced Monte Carlo methods for open systems: CFCMC vs CBMC. *J. Chem. Theory Comput.* **2014**, *10*, 942−952.

(96) Hens, R.; Rahbari, A.; Caro-Ortiz, S.; Dawass, N.; Erdős, M.; Poursaeidesfahani, A.; Salehi, H. S.; Celebi, A. T.; Ramdin, M.; Moultos, O. A.; Dubbeldam, D.; Vlugt, T. J. H. Brick-CFCMC: Open source software for Monte Carlo simulations of phase and reaction equilibria using the Continuous Fractional Component Method. *J. Chem. Inf. Model.* **2020**, *60*, 2678−2682.

(97) Bueno-Pérez, R.; Calero, S.; Dubbeldam, D.; Ania, C. O.; Parra, J. B.; Zaderenko, A. P.; Merkling, P. J. Zeolite force fields and experimental siliceous frameworks in a comparative infrared study. *J. Phys. Chem. C* **2012**, *116*, 25797−25805.

(98) Guo, J.; Hammond, K. D. Comparison of siliceous zeolite potentials from the perspective of infrared spectroscopy. *J. Phys. Chem. C* **2018**, *122*, 6093−6102.

(99) van Beest, B. W. H.; Kramer, G. J.; van Santen, R. A. Force fields for silicas and aluminophosphates based on ab initio calculations. *Phys. Rev. Lett.* **1990**, *64*, 1955−1958.

(100) Kramer, G. J.; Farragher, N. P.; van Beest, B. W. H.; van Santen, R. A. Interatomic force fields for silicas, aluminophosphates, and zeolites: Derivation based on ab initio calculations. *Phys. Rev. B* **1991**, *43*, 5068−5080.

(101) Hill, J.-R.; Sauer, J. Molecular mechanics potential for silica and zeolite catalysts based on ab initio calculations. 2. aluminosilicates. *J. Phys. Chem.* **1995**, *99*, 9536−9550.

(102) Demontis, P.; Suffritti, G. B.; Quartieri, S.; Fois, E. S.; Gamba, A. Molecular dynamics studies on zeolites. II: A simple model for silicates applied to anhydrous natrolite. *Zeolites* **1987**, *7*, 522−527.

(103) Demontis, P.; Suffritti, G. B.; Quartieri, S.; Fois, E. S.; Gamba, A. Molecular dynamics studies on zeolites. 3. Dehydrated zeolite A. *J. Phys. Chem.* **1988**, *92*, 867−871.

(104) Demontis, P.; Suffritti, G. B.; Fois, E. S.; Gamba, A.; Morosi, G. A potential for molecular dynamics simulations of structural and dynamic properties of hydrate aluminosilicates. *Mater. Chem. Phys.* **1991**, *29*, 357−367.

(105) Nicholas, J. B.; Hopfinger, A. J.; Trouw, F. R.; Iton, L. E. Molecular modeling of zeolite structure. 2. Structure and dynamics of silica sodalite and silicate force field. *J. Am. Chem. Soc.* **1991**, *113*, 4792−4800.

(106) Gabrieli, A.; Sant, M.; Demontis, P.; Suffritti, G. B. Development and optimization of a new force field for flexible aluminosilicates, enabling fast molecular dynamics simulations on parallel architectures. *J. Phys. Chem. C* **2013**, *117*, 503−509.

(107) Ghysels, A.; Moors, S. L. C.; Hemelsoet, K.; De Wispelaere, K.; Waroquier, M.; Sastre, G.; Van Speybroeck, V. Shape-selective diffusion of olefins in 8-ring solid acid microporous zeolites. *J. Phys. Chem. C* **2015**, *119*, 23721−23734.

(108) Demontis, P.; Suffritti, G. B. Structure and dynamics of zeolites investigated by molecular dynamics. *Chem. Rev.* **1997**, *97*, 2845−2878.

(109) Toda, J.; Corma, A.; Abudawoud, R. H.; Elanany, M. S.; Al-Zahrani, I. M.; Sastre, G. Influence of force fields on the selective diffusion of para-xylene over ortho-xylene in 10-ring zeolites. *Mol. Simul.* **2015**, *41*, 1438−1448.

(110) Sastre, G.; Kärger, J.; Ruthven, D. M. Molecular dynamics study of diffusion and surface permeation of benzene in silicalite. *J. Phys. Chem. C* **2018**, *122*, 7217−7225.

(111) Dick, B. G., Jr.; Overhauser, A. W. Theory of the dielectric constants of alkali halide crystals. *Phys. Rev.* **1958**, *112*, 90−103.

(112) Schröder, K.-P.; Sauer, J. Potential functions for silica and zeolite catalysts based on ab initio calculations. 3. A shell model ion

pair potential for silica and aluminosilicates. *J. Phys. Chem.* **1996**, *100*, 11043−11049.

(113) Sanders, M. J.; Leslie, M.; Catlow, C. R. A. Interatomic potentials for SiO$_2$. *J. Chem. Soc., Chem. Commun.* **1984**, 1271−1273.

(114) Sierka, M.; Sauer, J. Structure and reactivity of silica and zeolite catalysts by a combined quantum mechanics-shell-model potential approach based on DFT. *Faraday Discuss.* **1997**, *106*, 41−62.

(115) Henson, N. J.; Cheetham, A. K.; Gale, J. D. Theoretical calculations on silica frameworks and their correlation with experiment. *Chem. Mater.* **1994**, *6*, 1647−1650.

(116) Baker, J. An algorithm for the location of transition states. *J. Comput. Chem.* **1986**, *7*, 385−395.

(117) Banerjee, A.; Adams, N.; Simons, J.; Shepard, R. Search for stationary points on surfaces. *J. Phys. Chem.* **1985**, *89*, 52−57.

(118) Gelb, L. D.; Gubbins, K. E. Pore size distributions in porous glasses: A computer simulation study. *Langmuir* **1999**, *15*, 305−308.

(119) Sarkisov, L.; Harrison, A. Computational structure characterisation tools in application to ordered and disordered porous materials. *Mol. Simul.* **2011**, *37*, 1248−1257.

(120) Widom, B. Some topics in the theory of fluids. *J. Chem. Phys.* **1963**, *39*, 2808−2812.

(121) Bezus, A. G.; Kiselev, A. V.; Lopatkin, A. A.; Du, P. Q. Molecular statistical calculation of the thermodynamic adsorption characteristics of zeolites using the atom-atom approximation. Part 1.- Adsorption of methane by zeolite NaX. *J. Chem. Soc. Faraday Trans. 2* **1978**, *74*, 367−379.

(122) Pascual, P.; Ungerer, P.; Tavitian, B.; Pernot, P.; Boutin, A. Development of a transferable guest-host force field for adsorption of hydrocarbons in zeolites I. Reinvestigation of alkane adsorption in silicalite by grand canonical Monte Carlo simulation. *Phys. Chem. Chem. Phys.* **2003**, *5*, 3684−3693.

(123) Pascual, P.; Ungerer, P.; Tavitian, B.; Boutin, A. Development of a transferable guest-host force field for adsorption of hydrocarbons in zeolites. II. Prediction of alkenes adsorption and alkane/alkene selectivity in silicalite. *J. Phys Chem. B* **2004**, *108*, 393−398.

(124) Dubbeldam, D.; Calero, S.; Vlugt, T. J. H.; Krishna, R.; Maesen, T. L. M.; Smit, B. United atom force field for alkanes in nanoporous materials. *J. Phys. Chem. B* **2004**, *108*, 12301−12313.

(125) Liu, B.; Smit, B.; Rey, F.; Valencia, S.; Calero, S. A new united atom force field for adsorption of alkenes in zeolites. *J. Phys. Chem. C* **2008**, *112*, 2492−2498.

(126) Bai, P.; Tsapatsis, M.; Siepmann, J. I. TraPPE-zeo: Transferable potentials for phase equilibria force field for all-silica zeolites. *J. Phys. Chem. C* **2013**, *117*, 24375−24387.

(127) García-Sánchez, A.; Ania, C. O.; Parra, J. B.; Dubbeldam, D.; Vlugt, T. J. H.; Krishna, R.; Calero, S. Transferable force field for carbon dioxide adsorption in zeolites. *J. Phys. Chem. C* **2009**, *113*, 8814−8820.

(128) Wolffis, J. J.; Vanpoucke, D. E. P.; Sharma, A.; Lawler, K. V.; Forster, P. M. Predicting partial atomic charges in siliceous zeolites. *Microporous Mesoporous Mater.* **2019**, *277*, 184−196.

(129) Abdelrasoul, A.; Zhang, H.; Cheng, C.-H.; Doan, H. Applications of molecular simulations for separation and adsorption in zeolites. *Microporous Mesoporous Mater.* **2017**, *242*, 294−348.

(130) Desbiens, N.; Boutin, A.; Demachy, I. Water condensation in hydrophobic silicalite-1 zeolite: A molecular simulation study. *J. Phys. Chem. B* **2005**, *109*, 24071−24076.

(131) Caro-Ortiz, S.; Hens, R.; Zuidema, E.; Rigutto, M.; Dubbeldam, D.; Vlugt, T. J. H. Molecular simulation of the vapor-liquid equilibria of xylene mixtures: Force field performance, and Wolf vs. Ewald for electrostatic interactions. *Fluid Phase Equilibr.* **2019**, *485*, 239−247.

(132) Caro-Ortiz, S.; Hens, R.; Zuidema, E.; Rigutto, M.; Dubbeldam, D.; Vlugt, T. J. H. Corrigendum to "Molecular simulation of the vapor-liquid equilibria of xylene mixtures: Force field performance, and Wolf vs. Ewald for electrostatic Interactions" [Fluid Phase Equilib.] 485 (2019) 239-247. *Fluid Phase Equilibr.* **2020**, *506*, 112370.

(133) Rai, N.; Siepmann, J. I. Transferable potentials for phase equilibria. 9. Explicit hydrogen description of benzene and five-membered and six-membered heterocyclic aromatic compounds. *J. Phys. Chem. B* **2007**, *111*, 10790−10799.

(134) Rai, N.; Siepmann, J. I. Transferable potentials for phase equilibria. 10. Explicit-hydrogen description of substituted benzenes and polycyclic aromatic compounds. *J. Phys. Chem. B* **2013**, *117*, 273−288.

(135) Bonnaud, P.; Nieto-Draghi, C.; Ungerer, P. Anisotropic united atom model including the electrostatic interactions of benzene. *J. Phys. Chem. B* **2007**, *111*, 3730−3741.

(136) Nieto-Draghi, C.; Bonnaud, P.; Ungerer, P. Anisotropic united atom model including the electrostatic interactions of methylbenzenes. I. Thermodynamic and structural properties. *J. Phys. Chem. C* **2007**, *111*, 15686−15699.

(137) Nieto-Draghi, C.; Bonnaud, P.; Ungerer, P. Anisotropic united atom model including the electrostatic interactions of methylbenzenes. II. Transport properties. *J. Phys. Chem. C* **2007**, *111*, 15942−15951.

(138) Jorgensen, W. L.; Laird, E. R.; Nguyen, T. B.; Tirado-Rives, J. Monte Carlo simulations of pure liquid substituted benzenes with OPLS potential functions. *J. Comput. Chem.* **1993**, *14*, 206−215.

(139) Jorgensen, W. L.; Maxwell, D. S.; Tirado-Rives, J. Development and testing of the OPLS all-atom force field on conformational energetics and properties of organic liquids. *J. Am. Chem. Soc.* **1996**, *118*, 11225−11236.

(140) Cacelli, I.; Cinacchi, G.; Prampolini, G.; Tani, A. Computer simulation of solid and liquid benzene with an atomistic interaction potential derived from ab initio calculations. *J. Am. Chem. Soc.* **2004**, *126*, 14278−14286.

(141) Lopes, P. E. M.; Lamoureux, G.; Roux, B.; MacKerell, A. D. Polarizable empirical force field for aromatic compounds based on the classical Drude oscillator. *J. Phys. Chem. B* **2007**, *111*, 2873−2885.

(142) Sun, H. COMPASS: An ab initio force-field optimized for condensed-phase applications-Overview with details on alkane and benzene compounds. *J. Phys. Chem. B* **1998**, *102*, 7338−7364.

(143) Visscher, K. M.; Geerke, D. P. Deriving force-field parameters from first principles using a polarizable and higher order dispersion model. *J. Chem. Theory Comput.* **2019**, *15*, 1875−1883.

(144) Snurr, R. Q.; Bell, A. T.; Theodorou, D. N. A hierarchical atomistic/lattice simulation approach for the prediction of adsorption thermodynamics of benzene in silicalite. *J. Phys. Chem.* **1994**, *98*, 5111−5119.

(145) Wick, C. D.; Martin, M. G.; Siepmann, J. I. Transferable potentials for phase equilibria. 4. United-atom description of linear and branched alkenes and alkylbenzenes. *J. Phys. Chem. B* **2000**, *104*, 8008−8016.

(146) Martin, M. G.; Siepmann, J. I. Transferable potentials for phase equilibria. 1. United-atom description of n-alkanes. *J. Phys. Chem. B* **1998**, *102*, 2569−2577.

(147) Sun, M. S.; Talu, O.; Shah, D. B. Adsorption equilibria of C$_5$-C$_{10}$ normal alkanes in silicalite crystals. *J. Phys. Chem.* **1996**, *100*, 17276−17280.

(148) Choudhary, V. R.; Srinivasan, K. R. Sorption and diffusion of benzene in H-ZSM-5: Effect of SiAl ratio, degree of cation exchange and pretreatment conditions. *J. Catal.* **1986**, *102*, 328−337.

(149) Guo, G.-Q.; Chen, H.; Long, Y.-C. Separation of p-xylene from C$_8$ aromatics on binder-free hydrophobic adsorbent of MFI zeolite. I. Studies on static equilibrium. *Microporous Mesoporous Mater.* **2000**, *39*, 149−161.

(150) Derouane, E. G. Shape selectivity in catalysis by zeolites: The nest effect. *J. Catal.* **1986**, *100*, 541−544.

(151) Sastre, G.; Corma, A. The confinement effect in zeolites. *J. Mol. Catal. A: Chem.* **2009**, *305*, 3−7.

(152) Lipkowitz, K. B.; Peterson, M. A. Benzene is not very rigid. *J. Comput. Chem.* **1993**, *14*, 121−125.

(153) Laaksonen, A.; Wang, J.; Boyd, R. J. Internal motion of benzene. A molecular dynamics simulation study. *Chem. Phys. Lett.* **1995**, *241*, 380−386.

(154) Ruthven, D. M.; Eic, M.; Richard, E. Diffusion of C_8 aromatic hydrocarbons in silicalite. *Zeolites* **1991**, *11*, 647−653.

(155) Kärger, J.; Ruthven, D. M. *Diffusion in zeolites and other microporous solids*; 1st ed.; Wiley-Interscience: 1992.